Article

Not peer-reviewed version

Intelligent Temperature Control Using Artificial Neural Networks in an IoT-Enabled Cyber-Physical Hot-Air Drying System: Analysis of Drying Kinetics and Thermal Efficiency

Juan Manuel Tabares-Martinez , Adriana Guzmán-López * , Micael Gerardo Bravo-Sánchez * , Francisco Villaseñor-Ortega , Juan José Martínez-Nolasco , Alejandro Israel Barranco-Gutierrez

Posted Date: 27 February 2026

doi: 10.20944/preprints202602.1525.v1

Keywords: artificial neural networks; IoT; cyber-physical system; Arduino Mega 2560; hot-air drying; drying kinetics; thermal efficiency

 doi:10.20944/preprints202602.1525.v1

Article

Intelligent Temperature Control Using Artificial Neural Networks in an IoT-Enabled Cyber-Physical Hot-Air Drying System: Analysis of Drying Kinetics and Thermal Efficiency

Juan Manuel Tabares-Martinez [1], Adriana Guzmán-López [2,*], Micael Gerardo Bravo-Sánchez [2,*], Francisco Villaseñor-Ortega [2], Juan José Martínez-Nolasco [3] and Alejandro Israel Barranco-Gutierrez [4]

[1] Departamento de Posgrado e Investigación (DEPI), Tecnológico Nacional de México (TecNM), Instituto Tecnológico de Celaya (ITC), Celaya, Guanajuato 38010, México
[2] Departamento de Ingeniería Bioquímica e Ingeniería Ambiental, Tecnológico Nacional de México (TecNM), Instituto Tecnológico de Celaya (ITC), Celaya, Guanajuato 38010, México
[3] Departamento de Ingeniería Mecatrónica, Tecnológico Nacional de México (TecNM), Instituto Tecnológico de Celaya (ITC), Celaya, Guanajuato 38010, México
[4] Departamento de Ingeniería Electrónica, Tecnológico Nacional de México (TecNM), Instituto Tecnológico de Celaya (ITC), Celaya, Guanajuato 38010, México
* Correspondence: adriana.guzman@itcelaya.edu.mx (A.G.-L.); gerardo.bravo@itcelaya.edu.mx (M.G.B.-S.)

Abstract

A control algorithm based on artificial neural networks was developed to regulate the hot-air drying temperature for carrot dehydration within an IoT-enabled cyber-physical system. The experimental setup employs an Arduino Mega 2560 equipped with AM2302, MLX90614, and SHT35 sensors, an HX711 load cell, and a WS68 anemometer, with cloud communication provided by an ESP8266 module for remote monitoring via Wi-Fi under an IoT framework. The neural controller, implemented using the Arduino Neurona library, adjusts the dryer temperature in real time, ensuring thermal stability throughout operation. Three initial loads (2, 4, and 6 kg) were analyzed to obtain the drying kinetics and determine the thermal efficiency. In the dehydration experiments, the 2 kg load reached a final moisture content of 10% in 4.4 h, consuming 1,390 kJ with a thermal efficiency of 83%. The 4 kg load exhibited the best time–energy balance (6.6 h, 1,850.0 kJ, 88%), while the 6 kg load achieved the highest efficiency (8.1 h, 2,250.0 kJ, 91%). These results demonstrate the effectiveness of neural-network-based control implemented on low-cost microcontrollers to enhance thermal efficiency in food dehydration processes.

Keywords: artificial neural networks; IoT; cyber-physical system; Arduino Mega 2560; hot-air drying; drying kinetics; thermal efficiency

1. Introduction

The removal of moisture from foods through hot-air drying constitutes one of the most widely employed technologies at the industrial and agro-industrial levels for the preservation of perishable products, due to its relative operational simplicity, low implementation cost, and ability to significantly extend shelf life by reducing water activity. This process is particularly attractive in the food industry, where microbiological stability, the reduction of postharvest losses, and the preservation of sensory and nutritional attributes are critical factors for the competitiveness and sustainability of production systems [1]. The kinetics of moisture removal are highly dependent on the type of food, thermal conditions, and the mechanisms of heat and mass transfer, which has

 doi:10.20944/preprints202602.1525.v1

motivated the development of advanced monitoring and modeling techniques for the drying process [2].

Continuous monitoring of moisture loss during the dehydration process has proven to be an effective tool for more accurately describing drying dynamics and improving the prediction of material behavior, particularly when advanced sensing methods are combined with neural network-based models capable of capturing complex nonlinear relationships [3]. Studies focused on products such as carrot have shown that optimizing hot-air drying conditions has a direct impact on both the dehydration rate and process efficiency, as well as on the final quality of the product, highlighting the need for control and optimization strategies that simultaneously consider multiple process objectives [4].

Hot-air convective drying is intrinsically a highly energy-intensive process, accounting for a significant fraction of the total energy consumption in food processing plants, which depends on both the type of product and the operational conditions of the process. This challenge is compounded by the physical complexity of drying, characterized by the simultaneous occurrence of heat and mass transfer phenomena, internal thermal gradients, moisture diffusion, material shrinkage, and structural changes in the food matrix, which collectively render drying a strongly nonlinear, coupled, and time-dependent dynamic system [5]. These nonlinearities have motivated the use of advanced models based on artificial intelligence and machine learning to describe and predict the physicochemical behavior of products during dehydration, particularly in assisted convective processes where thermal and process variables exhibit a high degree of interaction [6]. Neural network-based control approaches have further demonstrated their ability to anticipate quality changes in dehydrated foods, such as color variations and structural properties, reinforcing the relevance of intelligent techniques for the analysis and control of nonlinear drying processes [7].

Carrot (*Daucus carota* L.), used both for direct consumption and in industrial formulations, presents additional challenges during the drying process associated with the heterogeneity of plant tissue, variability in initial moisture content, structural anisotropy, and the thermal sensitivity of bioactive compounds such as carotenoids, vitamins, and sugars [8]. During drying, inadequate regulation of air temperature may lead to thermal degradation, non-enzymatic browning, loss of rehydration capacity, and deterioration of texture, as well as an unnecessary increase in energy consumption, which has motivated the adoption of intelligent models for predicting moisture diffusivity and specific energy consumption in convective drying processes [9]. Intelligent management of drying temperature has therefore become a key factor in simultaneously improving final product quality and process thermal performance [10].

Drying systems have traditionally been regulated using conventional control strategies. Although these methods are widely adopted due to their simplicity and ease of implementation, they exhibit significant limitations when applied to complex and nonlinear processes such as convective food drying, whose kinetics and thermal behavior depend on multiple coupled variables [11]. In particular, linear controllers require simplified system models and show reduced performance in the presence of external disturbances, load variations, changes in drying kinetics, and time-varying thermal dynamics throughout the process, which has encouraged the use of advanced models for the description and prediction of drying processes [12,13].

Artificial intelligence (AI) techniques have emerged as promising tools for the modeling, prediction, and control of nonlinear engineering processes, particularly in energy-optimized drying systems integrated with IoT technologies [14]. Among these techniques, artificial neural networks (ANNs) have demonstrated a remarkable ability to approximate complex nonlinear functions, learn implicit relationships between input and output variables, and adapt to dynamic systems without requiring an explicit mathematical formulation of the underlying physical process, as reported in the prediction of drying kinetics and physicochemical properties of food products. These characteristics make neural networks well-suited for the control of highly coupled thermal processes, such as hot-air drying [15,16].

 doi:10.20944/preprints202602.1525.v1

The development of cyber–physical systems (CPS) has enabled an increasingly tight integration between the physical and digital domains, combining sensors, actuators, intelligent control algorithms, and real-time communication capabilities for the monitoring and control of thermal and energy-related processes. In this context, the Internet of Things (IoT) plays a fundamental role by enabling device connectivity, remote access to process data, and visualization through cloud-based platforms, thereby facilitating continuous supervision and data-driven decision-making [17]. The convergence of CPS, IoT, and artificial intelligence has given rise to a new generation of intelligent systems capable of autonomously monitoring, modeling, and optimizing industrial processes through predictive techniques for estimating thermal and moisture-related variables in complex systems [18,19].

In recent years, several studies have explored the application of artificial intelligence based techniques to food drying processes, including the use of fuzzy logic, hybrid neuro-fuzzy models, artificial neural networks, and evolutionary algorithms for exergy assessment, multi-objective optimization, and drying kinetics modeling across different thermal systems [20,21]. However, most of these approaches rely on high-computational-capacity hardware, such as industrial computers or a local server, which limits their scalability, increases implementation costs, and hinders their adoption in small- and medium-scale agro-industrial applications.

The implementation of neural controllers directly on low-cost microcontrollers remains an emerging research area. Executing neural networks on resource-constrained hardware imposes strict limitations in terms of memory, processing speed, and energy consumption, requiring careful design of both the neural model and the system architecture. Moreover, few studies simultaneously evaluate drying kinetics, energy consumption, and thermal efficiency under an embedded neural control scheme, particularly within IoT-enabled cyber-physical architecture, despite recent advances in accelerated moisture diffusion modeling using trained neural networks [22].

In this context, the present study proposes the development and evaluation of an IoT-enabled hot-air drying cyber-physical system, in which an intelligent temperature controller based on artificial neural networks is implemented directly on a low-cost Arduino Mega 2560 microcontroller, following recent neural modeling approaches applied to drying kinetics and product quality assessment [23]. The system integrates environmental and process sensors for the measurement of temperature, relative humidity, air velocity, and mass loss, providing a multivariable representation of the dynamic state of the drying process, consistent with strategies adopted in energy and exergy analyses of batch drying systems [24]. Remote communication is established through an ESP8266 module, enabling real-time monitoring via IoT platforms and facilitating subsequent data analysis, in accordance with modern supervisory and multivariate forecasting schemes in continuous industrial drying systems [25].

The neural controller, implemented using the Neurona library for Arduino, adjusts the thermal power of the heating system according to the instantaneous drying conditions, ensuring thermal stability, adaptive response to load variations, and energy-efficient operation. This approach is consistent with recent studies based on artificial neural networks and neuro-fuzzy models applied to the control and prediction of critical variables in complex thermal processes [26–28]. Unlike conventional strategies, neural inference is executed entirely at the microcontroller level, allowing the system to operate autonomously even in the absence of network connectivity, thereby enhancing its applicability in real agro-industrial environments where robust and low-computational-cost solutions are required.

The experimental study was conducted through the dehydration of carrots, aiming to analyze the drying kinetics, moisture removal rate, energy consumption, and thermal efficiency of the system under intelligent control. This methodology follows approaches similar to those employed in modeling dehydration kinetics using neural network-based techniques [29]. Evaluating the controller performance under different operating loads enables validation of its robustness and scalability, as well as the identification of the optimal trade-off between drying time and process efficiency.

 doi:10.20944/preprints202602.1525.v1

Accordingly, this study aims to bridge the existing gap between advanced artificial intelligence-based drying models and their practical implementation in resource-constrained agro-industrial environments by experimentally validating a fully embedded, IoT-enabled neural control strategy for convective food drying. The results of this work contribute to the advancement of intelligent drying technologies by demonstrating the feasibility of deploying neural network-based control, offering a scalable and sustainable solution aligned with current trends in smart agro-industrial automation and sustainability-oriented food processing.

2. Materials and Methods

The experiments were conducted in a controlled laboratory environment at the National Technological Institute of Mexico in Celaya, Guanajuato, during the period from January 2025 to January 2026. A hot-air convective drying system integrated into IoT-enabled cyber-physical architecture was employed for the experimental evaluation. Fresh carrots were used as the plant material, selected under homogeneous commercial conditions and characterized by high initial moisture content, making them a representative product for the analysis of thermal dehydration processes and the investigation of nonlinear drying kinetics.

The experimental system was designed to operate under an intelligent control scheme, in which temperature regulation is performed by an artificial neural network embedded in a low-cost microcontroller, following previously reported approaches for the modeling and prediction of critical variables in agricultural and industrial drying processes using artificial neural networks [30]. This configuration enabled continuous acquisition and real-time processing of thermal and process-related variables, as well as remote monitoring of the drying operation, with the aim of simultaneously evaluating moisture removal kinetics and the thermal performance of the system under different loading conditions [31].

2.1. Technical Specifications and Operational Features of the Convective Drying System

The dehydration process was conducted using a hot-air drying system consisting of a cylindrical drying chamber with a length of 0.35 m and an internal diameter of 0.30 m, designed to maintain stable thermal conditions and ensure uniform product distribution during operation. The drying chamber was arranged in a horizontal configuration, promoting homogeneous exposure to the hot airflow generated by a centrifugal fan with a maximum power rating of 200 W. This configuration has been reported as effective in enhancing convective heat transfer and minimizing temperature and moisture gradients in forced-convection drying processes, enabling operation within a temperature range of 55 °C to 85 °C [32].

Thermal energy was supplied by an electric heating element coupled to a forced ventilation system responsible for driving the heated air through the drying chamber. The heating power was dynamically regulated via a pulse-width modulation (PWM) signal generated by an intelligent controller, allowing precise and adaptive temperature control throughout the drying process. This control strategy is consistent with intelligent drying approaches aimed at reducing energy consumption and improving energy efficiency in agro-industrial drying systems [33]. The reference variable used for control corresponded to the temperature of the circulating air inside the chamber, providing a direct representation of the actual thermal environment to which the samples were exposed during dehydration. This system configuration is suitable for the simultaneous evaluation of moisture removal kinetics and the thermal performance of the dryer under different operating conditions.

The convective drying system developed in this study was designed to maintain precise, real-time control of critical dehydration process variables, including the air temperature within the chamber, relative humidity, airflow velocity, and product mass loss. Homogeneous exposure to the hot air minimizes temperature and moisture gradients, promoting uniform drying kinetics [34]. The distributed instrumentation and sensor integration enable the implementation of an embedded artificial neural network controller on a low-cost microcontroller, which dynamically adjusts the

 doi:10.20944/preprints202602.1525.v1

dryer's operational parameters to optimize drying efficiency and reduce process time [35]. Additionally, IoT connectivity facilitates multivariable data acquisition, providing real-time information for modeling drying kinetics and evaluating intelligent control strategies in agro-industrial cyber-physical systems [36]. This combination of intelligent control and continuous monitoring contributes to a robust and scalable dehydration process, particularly suitable for production environments with limited resources, as illustrated in Figure 1.

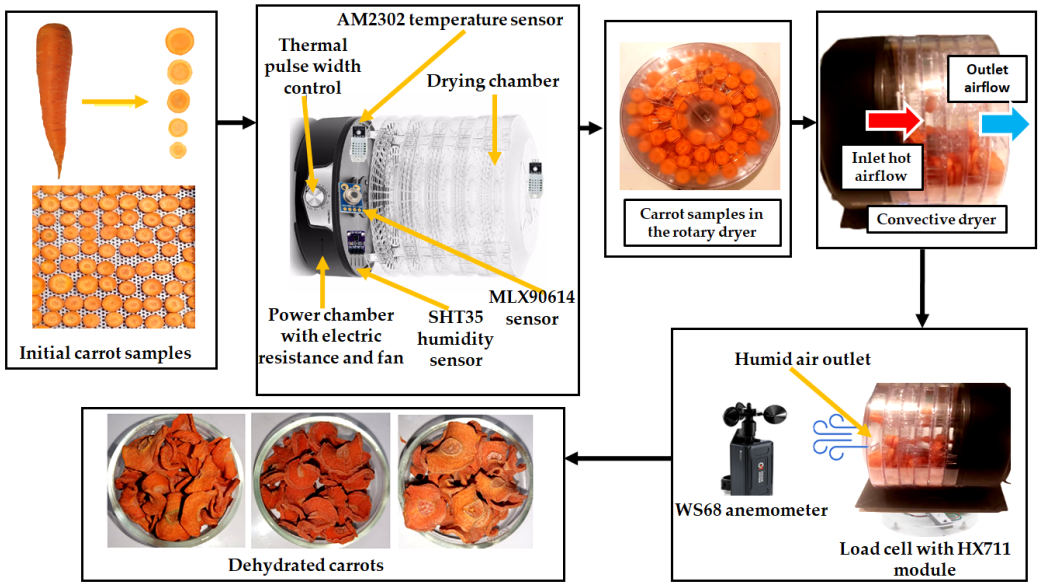

Figure 1. Experimental configuration of the convective carrot dehydration system.

2.2. Characterization of Samples and Thermal Conditions of the Drying Process

For the development of the experimental trials, fresh carrots were used, selected based on size uniformity and external physical condition in order to ensure comparable initial conditions among samples, as recommended in recent studies on drying kinetics and thermo-energetic modeling of agricultural products [37]. Prior to the dehydration process, the plant material was washed with potable water to remove surface impurities, mechanically peeled, and then sliced into discs with a controlled thickness of 6 ± 0.3 mm. The resulting slices exhibited an average major diameter of 3.8 cm and a minor diameter of 2.3 cm, dimensions commonly adopted to ensure representative heat and mass transfer during convective drying of root vegetables.

Before each experimental run, the samples were weighed and uniformly distributed inside the drying chamber to guarantee homogeneous exposure to the hot air flow and to minimize local variations in thermal conditions. The experiments were conducted under three different product load conditions (2 kg, 4 kg, and 6 kg) to analyze the influence of sample mass on drying behavior and moisture removal kinetics. All trials were performed under constant operating conditions, using an average drying air temperature of 76 °C and an air velocity of 1.6 m/s. These parameters were selected based on values reported as suitable for convective drying processes and intelligent drying systems incorporating advanced monitoring and control strategies [38].

2.3. Implementation of a Cyber-Physical Platform for Intelligent Control of Carrot Drying

The CPS was developed to enable continuous and real-time supervision of the key variables involved in the hot-air dehydration process through the integration of high-precision distributed electronic instrumentation. The surface temperature of the product was measured using an MLX90614 infrared sensor, while the air temperature inside the drying chamber was monitored using digital AM2302 sensors. The relative humidity of the drying air was recorded using an SHT35

 doi:10.20944/preprints202602.1525.v1

transducer, allowing a reliable characterization of the hygrothermal conditions throughout the operation. Airflow velocity was measured with a WS68 anemometer, and the mass variation of the product during drying was determined using load cells coupled to an HX711 analog to digital converter integrated into the data acquisition system, following approaches commonly adopted in IoT-based instrumented drying systems [39].

All sensor signals were conditioned and digitized using an Arduino Mega 2560 platform, selected for its processing capability, operational stability, and compatibility with multivariable data acquisition applications. This configuration minimized electrical interference and ensured the reliability of the recorded data, which were subsequently used for thermal efficiency analysis and dynamic performance evaluation of the drying process. In addition, the system incorporated an ESP8266 communication module to establish connectivity with the Arduino IoT Cloud platform, enabling remote monitoring, data storage, and real-time visualization of process variables within an IoT framework, consistent with smart drying architectures reported in recent literature [40].

The control strategy was implemented directly on the Arduino Mega platform, taking advantage of its capability to execute embedded intelligent control algorithms. Thermal regulation was achieved using an artificial neural network–based controller programmed in C++ through the Neurona library within the Arduino IDE, specifically designed for deploying neural models on resource-constrained microcontrollers. This architecture enabled the simultaneous monitoring of temperature, relative humidity, airflow velocity, and product mass loss, allowing dynamic adjustment of the dryer operating conditions according to the instantaneous state of the process, in line with intelligent control strategies applied to complex thermal systems [41]. As a result, the system exhibited adaptive responses to variations in critical process variables, contributing to a reduction in drying time, minimization of residual moisture zones, and improvement in specific energy consumption per kilogram of processed product.

During the experimental phase, the heating and ventilation systems were activated under controlled conditions, and hygrometric, aerodynamic, and mass-related variables were continuously recorded throughout each trial. The drying process was maintained until the samples reached a final moisture content equal to or below 10% on a wet basis, as verified by the IoT-enabled data acquisition system, while the embedded neural controller ensured thermal stability throughout the operation, following experimental protocols comparable to those employed in instrumented intelligent dryers [42]. Upon completion of each drying cycle and after cooling the drying chamber, the final product mass and specific energy consumption were determined in accordance with previously established experimental procedures for agro-food products with similar characteristics, as illustrated in Figure 2.

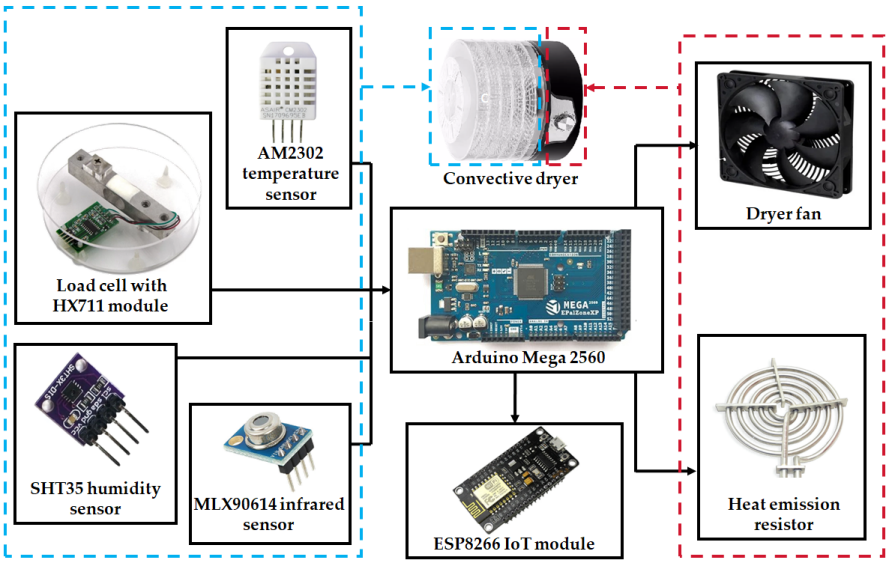

 doi:10.20944/preprints202602.1525.v1

Figure 2. Integration of sensors and microcontroller within the cyber-physical system for intelligent drying control.

2.4. Design and Implementation of the Embedded Artificial Neural Network Control for the Drying Process

The intelligent control strategy of the drying system is based on the implementation of an embedded artificial neural network (ANN) deployed on an Arduino Mega 2560 microcontroller, using the Neurona library within the Arduino IDE development environment. The implemented neural network corresponds to a feedforward multilayer perceptron, selected for its ability to approximate complex nonlinear relationships and for its suitability for real-time execution under the computational constraints inherent to low-cost embedded systems [43,44].

The final adopted architecture follows a 4–6–1 topology, consisting of an input layer with four neurons, a hidden layer with six neurons, and an output layer with a single neuron. This configuration represents an appropriate trade-off between generalization capability, numerical stability, and computational efficiency, ensuring robust performance during continuous operation of the drying system, as shown in Figure 3 [45].

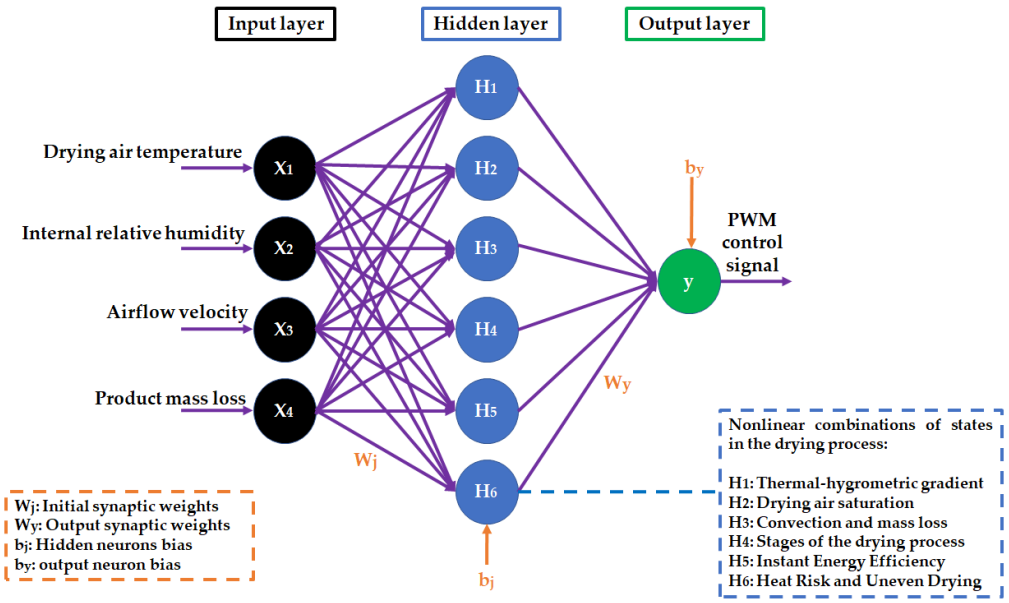

Figure 3. Multilayer perceptron type feedforward artificial neural network structure applied to temperature control using PWM.

2.4.1. Preprocessing and Normalization of Process Variables

Prior to neural processing, the signals acquired by the distributed instrumentation system are subjected to a normalization procedure, scaling the data to the operational range of the Neurona library, typically between 0 and 1. This preprocessing step is essential to improve numerical stability, reduce the likelihood of activation function saturation, and ensure consistent algorithmic behavior given the resolution and arithmetic precision limitations of microcontroller-based platforms [46].

Additionally, normalization homogenizes the scale of the input variables, preventing artificial dominance among physical parameters and promoting efficient information propagation throughout the neural network [47].

2.4.2. Training and Validation of the Neural Model

The neural network training was conducted externally (offline), using experimental data collected during preliminary drying trials performed under different operating conditions. This

 doi:10.20944/preprints202602.1525.v1

approach enabled the optimization of synaptic weights and bias terms through supervised learning techniques without imposing additional computational burdens on the embedded system [45,47].

Once the model performance was validated, the optimized parameters were directly embedded into the microcontroller code as fixed constants, allowing real-time neural inference without the need for online learning. This strategy significantly reduces memory usage and ensures stable and reproducible controller operation over extended periods of continuous use [48].

2.4.3. Selection and Definition of Input Variables

The input layer of the neural network is composed of four physical variables acquired in real time from the drying process: drying air temperature, internal relative humidity, airflow velocity, and instantaneous product mass loss. These variables collectively provide a comprehensive description of the thermodynamic and mass transfer state of the system, supplying sufficient information to characterize process dynamics while avoiding redundancy [49]. The input neurons do not perform internal computations; instead, they function as distribution nodes that transmit the normalized values to the hidden layer through weighted connections defined by the model parameters.

2.4.4. Configuration and Function of the Hidden Layer

The hidden layer of the neural network consists of six neurons, experimentally selected to adequately capture the nonlinear dynamics of convective drying without significantly increasing the computational load of the embedded system [47]. This layer concentrates the core processing of the neural model. Each hidden neuron computes a linear combination of the weighted inputs, followed by the application of a nonlinear activation function [49].

This mechanism enables the modeling of implicit physical phenomena within the drying process. The first hidden neuron captures the nonlinear interaction between drying air temperature and the internal relative humidity of the chamber, variables that determine the vapor pressure gradient responsible for surface evaporation. Experimentally, it was observed that temperature increments up to approximately 76 °C produce progressive reductions in relative humidity; however, this relationship does not exhibit linear behavior throughout the process. During the initial stage, intense evaporation maintains high relative humidity levels; in intermediate stages, small thermal increments lead to significant humidity reductions; whereas in the final stage, the thermal effect becomes attenuated. In this context, this neuron is predominantly activated when an effective thermal gradient exists, indicating favorable conditions for simultaneous heat and mass transfer.

The second hidden neuron identifies hygrothermal saturation conditions of the drying air, particularly under high loading scenarios (4–6 kg), where relative humidity remains elevated for prolonged periods despite temperature increases. This behavior reflects a limitation in the air's capacity to absorb additional moisture, thereby reducing process efficiency. This neuron functions as a detector of proximity to psychrometric saturation, allowing the controller to avoid unnecessary increases in thermal power when mass transfer is restricted by adverse hygrometric conditions.

The third hidden neuron models the coupled relationship between airflow velocity and the product mass loss rate, associated with the convective mass transfer coefficient. Experimental trials demonstrated that at velocities close to 1.6 m/s, higher dehydration rates are achieved during the initial hours of the process; however, further increases in velocity do not yield proportional improvements, indicating operation near a convective optimum regime. This neuron is activated when airflow effectively contributes to moisture removal and attenuates its response as the system approaches an aerodynamic efficiency limit.

The fourth hidden neuron dynamically differentiates the characteristic phases of convective drying: the constant-rate period, dominated by surface evaporation, and the falling-rate period, governed by internal moisture diffusion. Experimentally, mass loss is high during the initial hours and progressively decreases even under constant temperature conditions. This neuron enables the

 doi:10.20944/preprints202602.1525.v1

controller to recognize the transient state of the process and adjust the thermal strategy according to the dominant drying stage, contributing to more precise and context-aware regulation.

The fifth hidden neuron integrates temperature, relative humidity, and mass loss information to implicitly estimate the instantaneous thermal efficiency of the system. Under conditions of high temperature combined with low moisture removal rates, its activation decreases, indicating inefficient energy utilization. Conversely, when thermal increments effectively translate into moisture removal, its response increases. This neuron contributes to process energy optimization, aligning with intelligent drying strategies aimed at minimizing energy consumption without compromising performance.

The sixth hidden neuron detects critical combinations associated with overheating risk or non-uniform drying, characterized by high temperature, low relative humidity, and reduced mass loss, which are typical of the final drying stages. Under these conditions, the product contains low residual moisture, and the continued application of high thermal power may induce surface hardening or undesirable internal gradients. This neuron operates as a preventive mechanism within the neural architecture, indirectly modulating the control signal to soften thermal action and preserve product quality.

These relationships are not explicitly defined through physical equations; instead, they are inferred during the training stage and subsequently embedded in the microcontroller through fixed parameter values [43].

2.4.5. Output Layer and Generation of the Thermal Control Signal

The output layer consists of a single neuron responsible for generating the continuous control signal applied to the thermal system. This neuron receives the activated outputs from the hidden layer and produces a normalized scalar value representing the optimal actuation level [45]. For each neuron, the linear combination of its inputs is computed according to Equation (1).

$$z_j = \sum_{i=1}^{n} w_{ij} x_i + b_j \tag{1}$$

where x_i denote the input variables of the process, which collectively characterize the thermo-hygrometric and transport conditions inside the drying chamber. The parameters w_{ij} correspond to the synaptic weights that quantify the relative influence and contribution of each input variable x_i on neuron j, thereby defining the strength of the interconnection within the network architecture. The term b_j represents the bias associated with neuron j, acting as an adjustable offset that shifts the activation threshold and enhances the model's flexibility by preventing structural constraints such as forcing the mapping through the origin. The variable z_j denotes the resulting weighted summation at neuron j, which constitutes the linear intermediate representation of the input space prior to the application of the nonlinear activation function [46]. The neuron output is obtained through a nonlinear activation function, according to Equation (2).

$$a_j = f(z_j) \tag{2}$$

where $f(z_j)$ corresponds to a sigmoid or hyperbolic tangent function, introducing nonlinearity to capture complex thermo-physical interactions inherent to convective drying. In the adopted 4–6–1 architecture, the hidden layer generates intermediate nonlinear representations of the system state [47]. The output neuron performs a second weighted combination, calculated by Equation (3).

$$y_{pwm} = f\left(\sum_{j=1}^{6} w_y a_j + b_y\right) \tag{3}$$

where a_j denote the activations of the hidden layer, w_y are the output-layer weights, b_y is the output bias and y_{pwm} represents the normalized control signal. The synaptic weights and bias terms were obtained through supervised offline training and subsequently embedded as fixed parameters

 doi:10.20944/preprints202602.1525.v1

in the microcontroller programmed using the Arduino IDE, enabling real-time inference without online retraining [48]. Finally, the normalized output is scaled to the actuator operating range (0–255) to generate the pulse-width modulation (PWM) signal, as described by Equation (4).

$$\mathrm{PWM} = 255 \cdot y_{pwm} \tag{4}$$

The PWM based actuation ensures smooth and stable thermal regulation of the drying air, closing the control loop in real time and enabling adaptive energy-efficient operation [50].

2.4.6. Application of the Control Signal and Closed-Loop Operation

During dryer operation, process variables are acquired in real time and introduced as inputs to the embedded neural network, with neural inference executed synchronously with sensor data acquisition. The output generated by the model is subsequently scaled to the physical range of the thermal actuator and applied directly to the heating system, thereby closing the control loop in real time [48].

This approach enables dynamic adaptation of the process temperature in response to simultaneous variations in hygrothermal conditions, aerodynamic parameters, and product state, without relying on explicit mathematical models of the drying process. As a result, enhanced thermal stability, improved adaptability to changes in product moisture content, and efficient operation under multiple loading conditions are achieved. All data acquisition, neural processing, and control signal generation tasks are executed locally on the microcontroller, ensuring low latency, high operational robustness, and feasibility for implementation in agro-industrial environments with multiple operational variables [43,49], as illustrated in Figure 4.

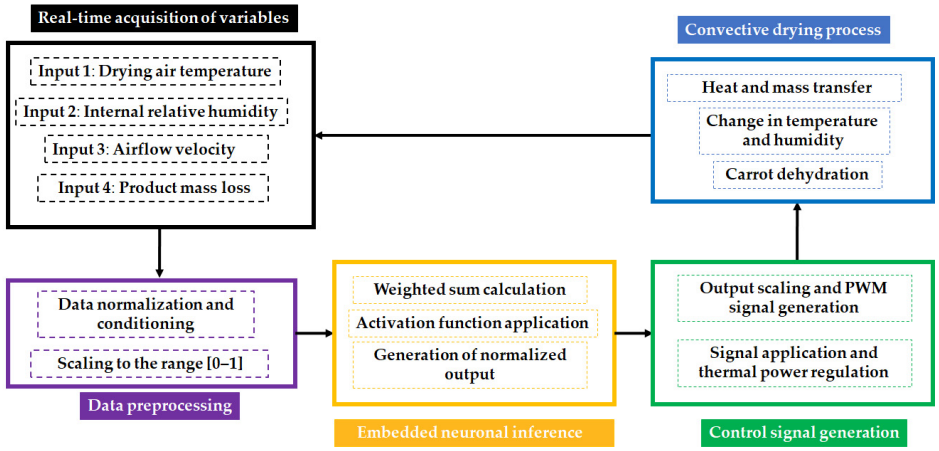

Figure 4. Integration of the Data Acquisition System, Neural Inference, and Closed-Loop Control Signal Generation.

2.5. IoT Implementation Using the ESP8266 Module in the Dehydration Process

To enable remote supervision, systematic data storage, and real-time visualization of the drying process variables, an IoT connectivity architecture based on the ESP8266 Wi-Fi module was implemented and integrated into the cyber-physical drying system as a communication interface. The selection of the ESP8266 was based on its low cost, low power consumption, integrated processing capability, and native compatibility with the Arduino IoT Cloud environment, making it a widely adopted solution for embedded monitoring and control applications in intelligent drying IoT systems [36,39,42].

The ESP8266 module was configured to establish wireless communication between the Arduino Mega 2560 board, responsible for data acquisition and execution of the embedded neural controller, and the Arduino IoT Cloud platform, which manages data visualization and storage. Communication

 doi:10.20944/preprints202602.1525.v1

between the microcontroller and the connectivity module was achieved through an asynchronous serial interface, ensuring reliable transmission of sensed data without interfering with the real-time execution of the artificial neural network–based control algorithm, as reported in distributed IoT-enabled cyber-physical drying systems [37,39].

Once connected to the local wireless network, the ESP8266 enabled continuous transmission of the process variables. This architecture allowed real-time monitoring of the dehydration process through the cloud platform, where instantaneous values and temporal evolution of critical variables were visualized, facilitating the analysis of the system's dynamic behavior under different operating conditions [36,42].

Additionally, the Arduino IoT Cloud platform was employed as an automatic data storage system, enabling the generation of structured historical records for subsequent offline analysis. These datasets were used for drying kinetics modeling, thermal efficiency evaluation, and energy performance assessment, in accordance with recent intelligent drying approaches that integrate energy analysis and data-driven modeling techniques [37,51,52]. The implementation of continuous data logging reduced manual intervention, minimized acquisition errors, and ensured data integrity during long-duration experimental trials.

The integration of the ESP8266 module within the cyber-physical system also enabled remote access to the drying system, allowing supervision of experimental runs without the need for constant physical presence in the laboratory. This capability enhances operational flexibility and aligns with the principles of Industry 4.0 and smart agro-industrial processing, where connectivity, digitalization, and process traceability are key elements for optimization and decision-making [36,39,52].

Finally, the combined application of distributed instrumentation embedded intelligent control, wireless communication, and cloud-based data analysis operates in an integrated manner within the proposed system. This architecture supports system scalability, facilitates multivariable data-driven analysis, and provides a robust framework for evaluating advanced intelligent control strategies in convective drying processes under real operating conditions, consistent with recent studies on IoT-assisted drying and advanced modeling using artificial neural networks, as illustrated in Figure 5 [37,53,54].

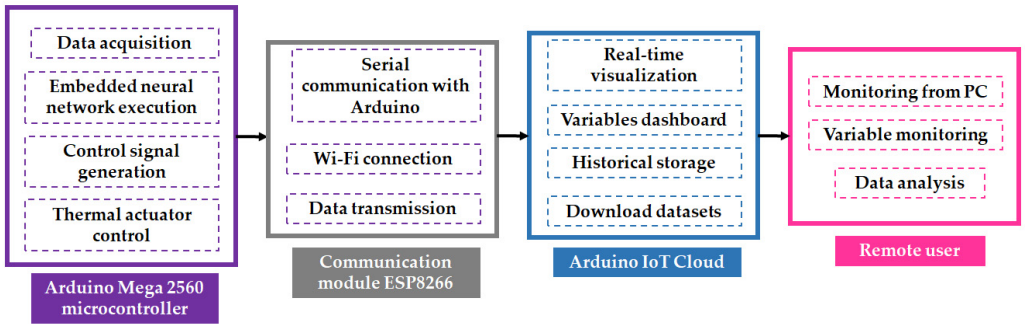

Figure 5. Architecture of the cyber-physical convective drying system with neural control for real-time monitoring and recording of variables.

2.6. Evaluation of the Total Energy Required in the Drying Process

During the experimental trials, the drying process of carrot samples was continuously monitored in the dryer with the aim of quantifying the energy demand of the system. Throughout the process, key variables such as the evolution of product mass and the thermal conditions of the system were recorded, enabling the estimation of fundamental parameters, including the energy required for moisture removal, the energy flux transferred from the hot air to the carrot samples, the

 doi:10.20944/preprints202602.1525.v1

dehydration rate, and the overall energy efficiency. These indicators constitute essential metrics for assessing the thermal performance of the proposed system [55,56].

The total heat required for the removal of moisture from the product (H_T, kJ) was determined by considering the energy contributions associated with heating the water contained within the carrot matrix and its subsequent vaporization. In this context, HT is expressed as the sum of the sensible heat required to raise the temperature of the carrot samples (H_{SC}) the energy associated with the preheating of water (H_{SW}), and the latent heat corresponding to the liquid–vapor phase change (H_L). This energy model enables a more accurate characterization of the heat transfer mechanisms involved in the drying process [57], as described in Equation (5).

$$H_T = H_{SC} + H_{SW} + H_L \quad (5)$$

The term associated with the sensible heating of the vegetal material (H_{SC}) quantifies the energy required to increase the temperature of the carrot from its initial condition to the thermal level established for the drying process, in accordance with the formulation described in Equation (6) [58].

$$H_{SC} = m_{ic} \cdot h_{sc}(T_c - T_d) \quad (6)$$

In this formulation, m_{ic} (kg) denotes the initial mass of the carrot samples, h_{sc} (kJ/kg°C) represents their specific heat capacity, T_c (°C) corresponds to the surface temperature of the product measured using the MLX90614 infrared sensor, and T_d (°C) denotes the average temperature inside the drying chamber, monitored through the AM2302 sensors.

The sensible heat of the water (H_{SW}) corresponds to the energy associated with the preheating of the water prior to the phase change. This energy contribution is calculated as a function of the mass of water present (m_w, kg), the specific heat capacity of water (h_{sw}, kJ/kg°C), and the temperature difference involved [57], as expressed in Equation (7).

$$H_{SW} = m_w \cdot h_{sw}(T_c - T_d) \quad (7)$$

The latent heat contribution (H_L) represents the energy demand associated with the phase transition of water from liquid to vapor during the carrot drying process. This term accounts for the evaporation of the moisture contained within the product matrix and is quantified using Equation (8), where m_{ew} (kg) denotes the mass of evaporated water and h_{lw} (kJ/kg) corresponds to the energy effectively consumed during the liquid–vapor phase change of water [58].

$$H_L = m_{ew} \cdot h_{lw} \quad (8)$$

The thermal energy transferred from the air stream to the carrot samples (H_A, kJ) was determined based on the thermophysical properties of the air and the operating conditions of the drying process, as described in Equation (9) [59]. In this formulation, D_a (kg/m³) represents the air density, h_a (kJ/kg·°C) its specific heat capacity, and T_{in} and T_{out} (°C) correspond to the inlet and outlet air temperatures of the system, respectively.

$$H_A = D_a \cdot E_V \cdot h_a(T_{in} - T_{out}) \quad (9)$$

The effective air volume processed by the drying system, E_V (m³), was estimated from the mean velocity of the convective air stream S_a (m/s), measured using a WS68 air velocity transducer, the cross-sectional area of the flow channel A_d (m²), and the effective operating time of the process T_t (s) [60,61]. This relationship, based on the volumetric balance of the convective flow, is expressed in Equation (10).

$$E_V = S_a \cdot A_d \cdot T_t \quad (10)$$

The moisture content of the product (M_c, % water content) was quantified using Equation (11). In this expression, m_d (kg) corresponds to the final dry-basis mass of the product. The estimation of this parameter enabled the characterization of moisture removal kinetics during the dehydration process [62].

$$M_c = \frac{m_{ic} - m_d}{m_{ic}} \times 100 \quad (11)$$

 doi:10.20944/preprints202602.1525.v1

The drying rate ($\dot{S}_d$, kg/h) was determined as the ratio between the total mass of water removed (m_{ew}, kg) and the effective drying time (T_t, h), as expressed in Equation (12). This parameter exhibited a progressive decline as the product moisture content approached the final dehydration condition, a behavior characteristic of the falling-rate period in convective drying processes. Experimental data acquired through load cells integrated with an HX711 module corroborated this trend, thereby validating the capability of the IoT-enabled cyber-physical system to stably regulate the drying process dynamics [63].

$$\dot{S}_d = \frac{m_{ew}}{T_t} \tag{12}$$

The thermal efficiency of the system (E_T, %) was estimated as the ratio between the energy required for the evaporation of moisture from the carrot samples (H_T, kJ) and the thermal energy transferred by the air stream during the drying process (H_A, kJ), according to Equation (13). This parameter quantifies the fraction of supplied energy effectively utilized for the evaporation phenomenon and represents an overall indicator of the dryer's energy performance; higher E_T values denote more efficient utilization of the energy input. Real-time monitoring of operational variables including air temperature, product surface temperature, convective airflow velocity, and product mass variation enabled the assessment of the system's thermal performance under different operating conditions [63,64].

$$E_T = \frac{H_T}{H_A} \times 100 \tag{13}$$

3. Results and Discussion

3.1. Analysis of Convective Drying Kinetics Under Embedded Neural Control

The drying kinetics of fresh carrot samples were analyzed in a convective hot-air dryer operating at an average temperature of 76 °C and a mean air velocity of 1.6 m/s, under the supervision of an IoT-based cyber-physical system implementing artificial neural network control. Air temperature was monitored using AM2302 sensors, airflow velocity was measured with a WS68 anemometer, and mass loss was recorded through load cells coupled with HX711 amplifiers. The acquired signals were processed by the microcontroller and transmitted via serial communication to the ESP8266 for real-time visualization and data storage through Arduino IoT Cloud, enabling continuous and synchronized monitoring of the process variables. This approach allowed the quantification of moisture removal dynamics and the evaluation of the influence of three initial loading masses (2 kg, 4 kg, and 6 kg) under controlled thermal conditions.

Moisture content reduction was determined from the experimentally recorded mass variation, and the moisture content was calculated using Equation (11), enabling the construction of the drying curves corresponding to each initial load. In all cases, the process was dominated by the falling-rate period, indicating that internal diffusion within the plant tissue was the primary mechanism governing moisture transport [1,3,5]. Increasing the initial mass resulted in a progressive decrease in the drying rate, which can be attributed to greater internal resistance to moisture movement within the dryer [4,6]. Figure 6 shows that the 2 kg load reached a final moisture content of 10% in 4.4 h, whereas the 4 kg and 6 kg loads required 6.6 h and 8.1 h, respectively.

The longer drying time observed for higher loads is associated with the increased total amount of water to be removed and with reduced efficiency in simultaneous heat and mass transfer, leading to higher internal moisture gradients [11,22]. Nevertheless, the embedded neural network controller maintained thermal stability throughout the process, compensating for the evaporative cooling effect associated with higher initial evaporation rates [28,48]. Compared with traditional solar drying or convective drying without intelligent control, the proposed system demonstrated improved responsiveness to operational variations and a reduction in total drying time, highlighting the effectiveness of the IoT-based cyber-physical approach for optimizing drying kinetics under controlled conditions [37,38,40].

 doi:10.20944/preprints202602.1525.v1

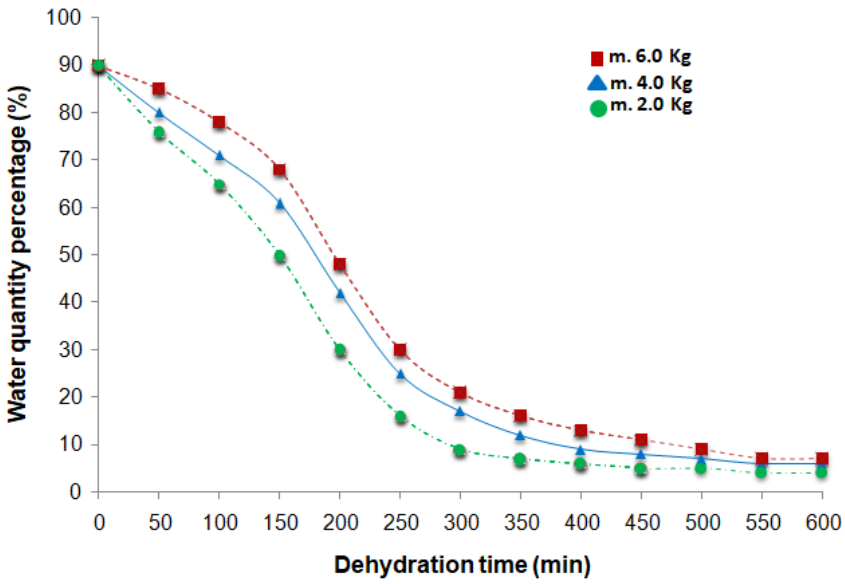

Figure 6. Evaluation of Drying Kinetics as a Function of the Initial Carrot Loading.

3.2. Thermal Monitoring Analysis During the Convective Drying Process

Thermal monitoring experiments were conducted to evaluate the temperature distribution dynamics inside the convective hot-air dryer operating under artificial neural network control. The objective was to characterize the thermal behavior of the drying chamber during carrot dehydration and to assess the system's ability to maintain stable and uniform temperature conditions under different initial product loads. Temperature measurements were performed using digital AM2302 sensors strategically installed within the drying chamber to ensure representative acquisition of the hot-air thermal field.

The temperature regulation strategy was based on a multilayer perceptron neural network embedded in the microcontroller. The output signal of the neural controller modulated the electrical heating element through an 8-bit PWM signal The output signal of the neural controller modulated the electric heating element through an 8-bit PWM signal and is calculated using Equations (1)–(4), allowing precise adjustment of the supplied thermal power. This closed-loop control architecture enabled dynamic compensation of disturbances associated with evaporative cooling and load-dependent thermal demand. As a result, temperature fluctuations commonly observed in conventional ON/OFF systems were significantly reduced, promoting a more stable thermal environment within the chamber and contributing to uniform moisture removal [43,47,48].

Experimental trials were performed with different initial product loads, maintaining an average chamber temperature of 76 °C during the active drying stage. As illustrated in Figure 7, a gradual temperature decrease to approximately 60 °C was observed when the product approached its final moisture content. This behavior is attributed to the reduction in evaporative demand as the available free water decreased, leading to lower latent heat consumption and a subsequent adjustment of the thermal equilibrium within the chamber. The neural controller responded adaptively to these variations, maintaining smooth thermal transitions without abrupt oscillations [31,55,65].

The selection of the digital AM2302 sensor provides several advantages compared with analog temperature sensors. Unlike the LM35, which requires analog-to-digital conversion and is more susceptible to electrical noise and signal degradation over longer transmission distances, the AM2302 delivers calibrated digital output signals, reducing measurement uncertainty and improving noise immunity. Its digital communication protocol enhances reliability in embedded and IoT-based environments, particularly in electrically noisy systems involving PWM-driven heating elements [14,23].

 doi:10.20944/preprints202602.1525.v1

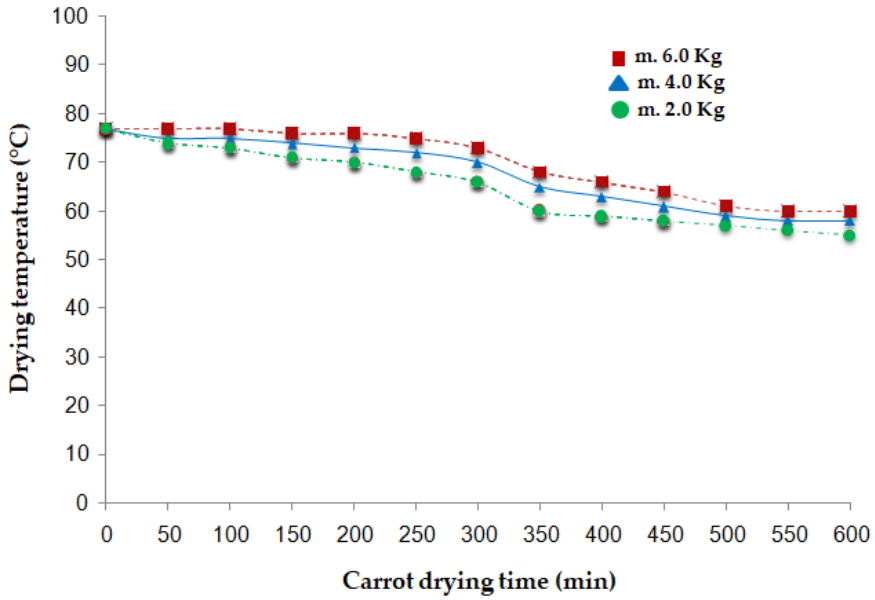

Figure 7. Thermal Behavior of the System during Convective Drying of Carrot.

The implementation of the IoT-based cyber-physical system with embedded neural temperature control offers significant advantages for precise thermal monitoring and regulation. First, it ensures real-time acquisition, processing, and cloud-based storage of temperature data, enabling traceability and post-process analysis. Second, the neural control strategy enhances thermal stability by adapting heater power continuously according to process conditions, minimizing overshoot and undershoot phenomena. Third, the integration of sensing, control, and wireless communication within a unified architecture improves operational robustness and facilitates remote supervision. Compared with conventional drying systems lacking intelligent control, this approach enhances temperature uniformity, reduces thermal stress on the product, contributes to improved energy efficiency and process reproducibility [24,35,37].

3.3. Evaluation of the Energy Supplied During the Drying Process

The energy supply in the convective hot-air dryer is directly associated with the simultaneous heat and mass transfer phenomena governing the dehydration of fresh carrots, which are characterized by a high initial moisture content. In this type of vegetable, most of the thermal energy supplied is initially used for the evaporation of free water and subsequently for the diffusion of bound moisture from the interior of the plant matrix toward the surface. Therefore, the energy input to the process depends not only on the magnitude of the heat flux delivered but also on its stability and proper spatial and temporal distribution within the drying chamber [1,5,11].

The thermal energy supplied to the process was determined using Equation (9), considering the operating conditions of the hot air and the thermodynamic parameters of the system. Experimental drying runs demonstrated that total energy consumption increased with the initial product mass, corresponding to the greater amount of water to be removed. For the 2 kg load, 1390 kJ were required to reach a final moisture content of 10%, whereas the 4 kg load demanded 1850 kJ and the 6 kg load required 2250 Kj, as illustrated in Figure 8. This behavior confirms the direct relationship between the supplied energy and the total amount of evaporated moisture, as well as the influence of internal mass transfer resistance at higher loading levels [11,22,24].

It is important to highlight that, despite the increased energy requirement for larger loads, the system achieved uniform drying without evidence of overheating, surface scorching, or structural degradation of the plant tissue. This indicates that energy was supplied in a controlled and

 doi:10.20944/preprints202602.1525.v1

progressive manner, preventing excessive thermal gradients that could compromise the final product quality [24,28].

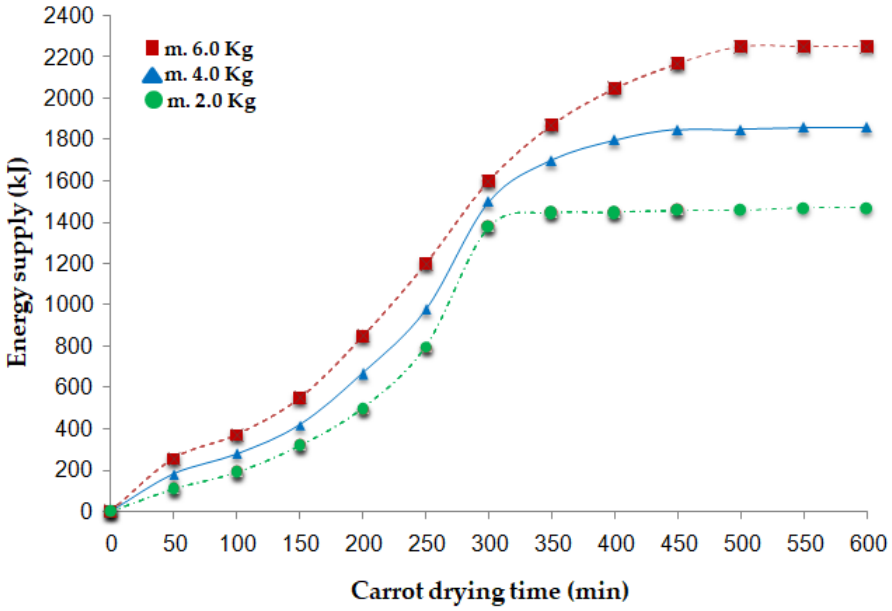

Figure 8. Profile of Thermal Energy Supplied by Hot-Air Flow during the Convective Dehydration of Carrot.

The implementation of an artificial neural network–based temperature control system had a direct impact on energy consumption optimization. Unlike conventional strategies such as PID or ON–OFF control, the neural controller dynamically adjusts the control signal according to the nonlinear behavior of the drying process, anticipating disturbances and compensating for phenomena such as evaporative cooling during the initial stages. This adaptive capability reduces abrupt thermal oscillations, minimizes overshoot peaks, and prevents repetitive on–off cycling that increases energy consumption and induces unnecessary thermal stress on the system [30,35,37].

In contrast, ON–OFF control systems tend to generate abrupt temperature fluctuations due to their binary nature, which may result in insufficient drying in certain product regions or thermal overexposure at the surface. Although PID control improves stability compared to ON–OFF systems, its performance may be limited in highly nonlinear and time-varying processes such as food drying, where optimal control parameters change as moisture content decreases [28,46,52].

The neural control strategy enabled efficient modulation of the hot-air flow and the supplied thermal power, adjusting the energy input according to the prevailing kinetic stage. As a result, a more rational use of energy was achieved, along with reduced thermal fluctuations and improved drying uniformity. Overall, the integration of intelligent control not only contributed to reaching the target moisture content with a lower risk of product deterioration, but also represented an effective approach for performing the energy balance of the convective dehydration process [15,24,35].

3.4. Analysis of the Drying Rate of Initial Carrot Loads

The drying rate is one of the most relevant kinetic parameters in the convective dehydration process of carrots, as it describes the rate of moisture removal from the product as a function of time and allows evaluation of the simultaneous efficiency of heat and mass transfer. In this study, the moisture removal rate was determined using Equation (12), based on the temporal variation of the recorded mass. Mass loss was measured in real time using load cells coupled with an HX711 amplifier module, enabling high-resolution quantification of the evaporated water throughout the entire drying process. This continuous monitoring strategy ensured an accurate and dynamic characterization of the dehydration process under controlled conditions [63,64,66].

 doi:10.20944/preprints202602.1525.v1

The experimental results showed that the 2 kg initial load exhibited an average drying rate of 0.409 kg/h, whereas the 4 kg load reached 0.545 kg/h and the largest load achieved an average rate of 0.667 kg/h. This behavior confirms that, in absolute terms, the moisture removal rate increases with the initial mass due to the greater total amount of water available for evaporation. However, increasing the load also implies a higher energy requirement, since water evaporation demands a thermal input proportional to the latent heat of vaporization in order to maintain the thermal balance through the vapor pressure gradient driving moisture migration. Additionally, sensible heat is required to raise the product temperature to conditions close to thermal equilibrium with the drying air [55,62,67].

The design of the convective dryer demonstrated an adequate response to variations in initial mass and moisture content, maintaining stability in the distribution of hot air within the chamber. Compared with traditional solar dryers, whose operation depends on variable climatic conditions and provides limited control over temperature and airflow, the intelligent-controlled convective system offers greater reproducibility and shorter drying times [57,58].

The neural network controller enabled anticipation of the reduction in the internal moisture gradient during the final stages of the process by modulating the supplied thermal power and stabilizing the drying rate. Figure 9 illustrates the evolution of the drying rate determined from mass loss as a function of drying time, highlighting the characteristic behavior of water removal and the influence of different initial loads on dehydration dynamics.

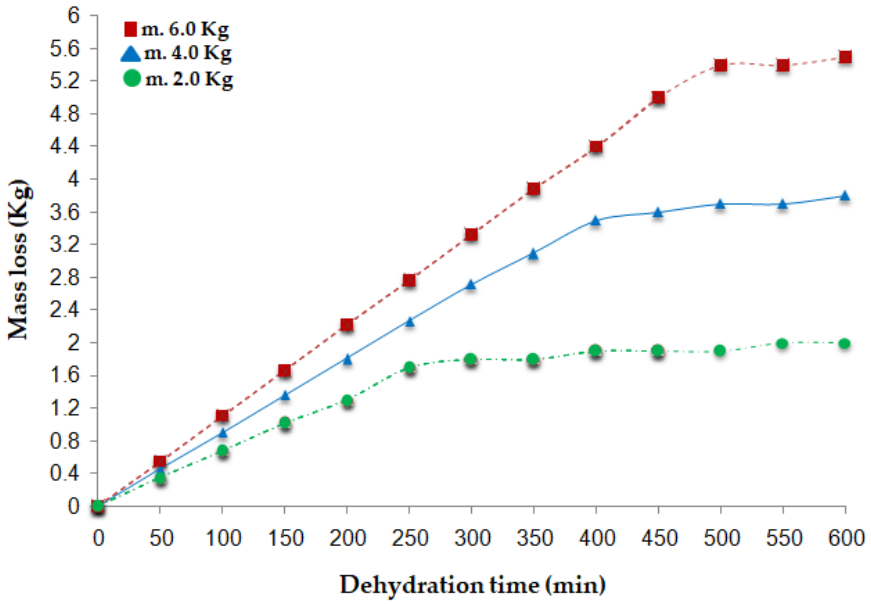

Figure 9. Temporal Evolution of Mass Loss through the Drying Rate during Convective Dehydration of Carrot.

3.5. Dynamics of Relative Humidity in the Convective Drying Chamber

Relative humidity (RH) inside the drying chamber is a key psychrometric parameter for evaluating the efficiency of the convective dehydration process, as it reflects the dynamic balance between moisture evaporation from the product and the capacity of the hot air to remove the generated vapor [68,69]. In this study, RH was monitored in real time using a digital SHT35 sensor integrated into the IoT-enabled cyber-physical system, allowing continuous and synchronized data acquisition throughout the entire experimental process.

The results showed that higher loads generated higher initial relative humidity values due to increased evaporation rates during the early stages of drying. The 2 kg load exhibited an initial RH inside the dryer cylinder of approximately 42%, whereas the 4 kg and 6 kg loads recorded values of about 48% and 55%, respectively. Subsequently, in all cases, a progressive decrease in RH was

 doi:10.20944/preprints202602.1525.v1

observed within the dryer, associated with the reduction of the product's moisture content and the predominance of the falling-rate period, during which internal diffusion governs moisture transport. When the carrot samples reached a final moisture content of 10%, the relative humidity stabilized at values close to 17–18%, indicating conditions near hygroscopic equilibrium under the controlled operating temperature, as illustrated in Figure 10 [37,48].

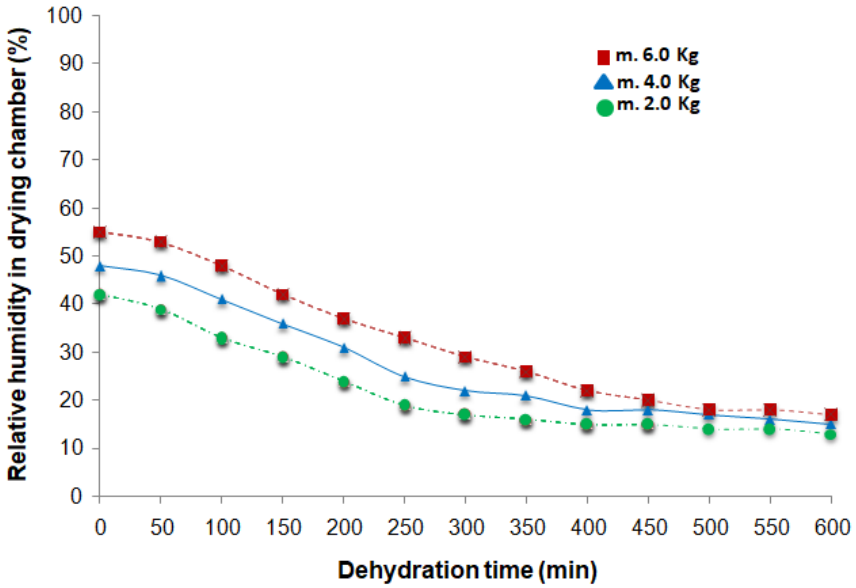

Figure 10. Real-Time Monitoring of Relative Humidity Dynamics inside the Convective Drying Chamber.

The stability of the relative humidity profiles confirms the effectiveness of the neural controller in regulating the drying chamber conditions, compensating for evaporative cooling effects. This intelligent regulation maintained a sustained vapor pressure gradient between the product and the surrounding air, thereby reducing the risk of localized rehydration or thermal overexposure [27,46,49].

3.6. Evaluation of Drying Efficiency of Carrots in the Convective Dehydrator

The thermal efficiency of the convective dryer represents an integral indicator of the system's energy performance, as it relates the useful energy employed for moisture evaporation from the product to the total energy supplied to the process. In this study, drying efficiency was determined using Equation (13), based on the energy balance between the heat required for water evaporation and the thermal energy delivered by the hot air stream. This approach enabled the quantification of the system's energy utilization under different initial loading conditions [70,71].

Experimental results demonstrated that thermal efficiency increased with the initial mass of the product. The 6 kg load achieved the highest efficiency (91%), whereas the 4 kg and 2 kg loads reached efficiencies of 88% and 83%, respectively, as shown in Figure 11. This behavior can be attributed to improved utilization of the supplied energy at higher product loads, since a larger amount of available moisture for evaporation reduces the relative thermal losses associated with heating the air and the dryer structure. In contrast, at lower loads, a greater fraction of the supplied energy is dissipated to the surroundings or consumed in heating the system components, thereby decreasing overall performance [68,72,73].

During the drying process, thermal efficiency did not remain strictly constant. Higher values were observed in the initial stages, when the evaporation rate was greater and most of the supplied energy was used as latent heat of vaporization. As the moisture content decreased and the process entered the falling-rate period, efficiency exhibited slight variations due to increased internal

 doi:10.20944/preprints202602.1525.v1

resistance to mass transfer. Nevertheless, the system maintained stable performance owing to the implemented thermal regulation strategy [11,15,23].

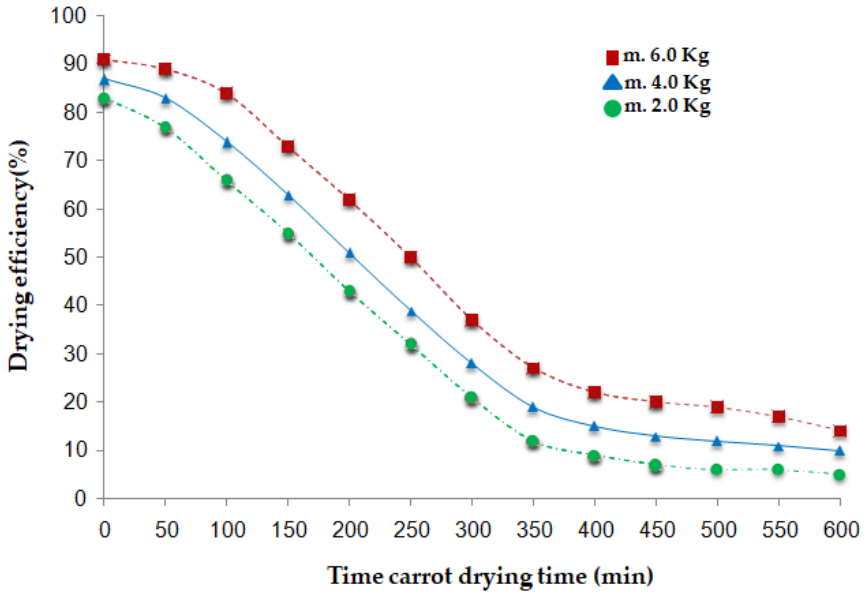

Figure 11. Thermal Efficiency of the Convective Dryer during the Carrot Dehydration Process under Different Initial Loading Conditions.

The implementation of a temperature controller based on a feedforward multilayer perceptron artificial neural network significantly contributed to the optimization of thermal efficiency. Unlike conventional control strategies, the neural controller adapted to the nonlinear behavior of the drying process and anticipated disturbances. This adaptive capability enabled continuous modulation of the supplied thermal power, minimizing energy losses and enhancing overall system efficiency [37,47,53].

4. Conclusions

The present study technically and scientifically validated the integration of IoT-based cyber–physical architecture with an artificial neural network (ANN)-based temperature controller in a convective dryer for carrot dehydration. Unlike previous research primarily focused on predictive modeling of drying kinetics using intelligent control approaches [10,13,15], this work implemented an embedded neural control scheme operating in real time, experimentally demonstrating its direct impact on thermal efficiency and process stability. The results confirmed that intelligent thermal regulation, supported by distributed sensing and continuous data acquisition, significantly enhances operational stability and energy utilization under different initial loading conditions [47,53,65].

The multilayer feedforward perceptron controller exhibited a strong adaptive capability in response to the nonlinear and dynamic behavior inherent to convective drying processes [22,24,46]. Continuous modulation of the supplied thermal power enabled the anticipation of variations associated with moisture content and internal mass transfer resistance, thereby reducing thermal oscillations and minimizing energy losses. This adaptive performance represents a clear advancement over conventional control strategies and is consistent with recent studies applying artificial intelligence for energy optimization in drying systems [20,24]. However, unlike those studies, the present research experimentally validates the integrated operation of neural control within a fully functional IoT architecture.

The implemented instrumentation constituted a fundamental pillar for system validation. Simultaneous monitoring of drying air temperature (AM2302), product surface temperature

 doi:10.20944/preprints202602.1525.v1

(MLX90614), relative humidity (SHT35), mass loss through load cells coupled with the HX711 module, and air velocity (WS68) enabled comprehensive characterization of heat and mass transfer phenomena. Cloud-based data transmission via the ESP8266 module ensured multivariable synchronization, in line with recent developments in IoT-based dehydration systems [36,39,70]. This integration not only enabled accurate calculation of thermal efficiency but also established a robust framework for real-time thermodynamic and energy analysis.

The thermal and hygrometric behavior inside the drying chamber confirmed system stability under neural control. Temperature remained within the optimal operating range, while relative humidity progressively decreased as drying advanced, indicating an adequate vapor pressure gradient for efficient moisture removal. This stable behavior ensured consistent operating conditions during the falling-rate period, where internal moisture diffusion resistance becomes dominant [22,46].

Furthermore, the analysis of different initial product masses demonstrated a direct relationship between loading capacity and thermal efficiency. Higher loads promoted improved energy utilization by allocating a larger fraction of the supplied energy to latent heat of vaporization, thereby reducing the relative impact of structural thermal losses. This finding is consistent with energy and exergy assessments reported in the literature [20,24,70].

From a methodological perspective, the combination of energy balance analysis, distributed sensing, adaptive control, and IoT infrastructure represents an integrated and replicable framework for the development of intelligent dryers aligned with Industry 4.0 principles [10,13]. The significance of this study lies in moving beyond isolated predictive modeling to demonstrate the practical implementation of a fully functional cyber–physical system with quantifiable improvements in energy efficiency and operational stability [15,47,53].

Overall, the results demonstrate that integrating artificial intelligence, multivariable monitoring, and cloud connectivity not only optimizes the thermal performance of convective dryers but also enhances system reliability, automation, and scalability. This work provides solid experimental evidence supporting the transition toward more energy-efficient, sustainable, and digitally integrated drying technologies, contributing to the advancement of intelligent drying systems based on adaptive control and real-time energy analysis.

Author Contributions: Conceptualization, J.M.T.-M. and M.G.B.-S.; methodology, J.M.T.-M., M.G.B.-S. and A.G.-L.; software, J.M.T.-M, J.J.M.-N. and A.I.B.-G.; validation, A.I.B.-G.; formal analysis, M.G.B.-S., A.G.-L., J.J.M.-N. and F.V.-O.; investigation, J.M.T.-M and M.G.B.-S.; resources,J.M.T.-M., A.G.-L., A.I.B.-G., F.V.-O. and J.J.M.-N.; writing—original draft preparation, J.M.T.-M., A.G.-L. and M.G.B.-S. .; writing—review and editing, J.M.T.-M. and M.G.B.-S.; supervision, A.G.-L., A.I.B.-G., J.J.M-N. and F.V.-O.; project administration, J.M.T.-M. and M.G.B.-S. All authors have read and agreed to the published version of the manuscript.

Funding: This research received no external funding.

Institutional Review Board Statement: Not applicable.

Informed Consent Statement: Not applicable.

Data Availability Statement: The original contributions presented in the study are included in the article.

Conflicts of Interest: The authors declare no conflicts of interest.

References

1. Demiray, E.; Özünlü, O.; Ergezer, H.; et al. Influence of Hot-Air Drying on the Drying Kinetics and Selected Quality Parameters of Sliced Chicken Breast Meat. *J. Therm. Anal. Calorim.* 2025, *150*, 13231–13241. https://doi.org/10.1007/s10973-025-14450-y
2. Ren, Y.; Zhu, X.; Tiwari, B.K.; Sun, D. Terahertz Time-Domain Spectroscopy Imaging Combined with Convolutional Long Short-Term Memory Neural Network for In Situ Moisture Reduction Prediction of

 doi:10.20944/preprints202602.1525.v1

Particle Foods during Pulsed Fluidized Bed Drying. *J. Food Eng.* 2024, *381*, 112183. https://doi.org/10.1016/j.jfoodeng.2024.112183

3. Fu, Y.; Zhang, Z.; Sun, D. Continuous Monitoring of Moisture Loss of Beef, Beetroot, and Banana Slices during Microwave Vacuum Dehydration Using THz-TDS Combined with a Transformer-Based Neural Network. *J. Food Eng.* 2025, *406*, 112774. https://doi.org/10.1016/j.jfoodeng.2025.112774
4. Geng, Z.; Torki, M.; Kaveh, M.; Beigi, M.; Yang, X. Characteristics and Multi-Objective Optimization of Carrot Dehydration in a Hybrid Infrared/Hot-Air Dryer. *LWT* 2022, *172*, 114229. https://doi.org/10.1016/j.lwt.2022.114229.
5. Ning, Z.; Khir, R.; Niederholzer, F.; Pan, Z. Characteristics of Moisture Diffusivity and Shrinkage Evolution of In-Hull Almonds under Hot-Air Drying. *LWT* 2025, *232*, 118455. https://doi.org/10.1016/j.lwt.2025.118455
6. El-Mesery, H.S.; Jibril, A.N.; ElMesiry, A.H.; Hu, Z.; Zhang, X.; Mahdi, A.A. Artificial Neural Network and Machine Learning Predictive Model for Assessing Physicochemical Properties of Garlic Slices (*Allium sativum* L.) during Microwave-Assisted Convective Drying Process. *Food Chemistry X* 2025, *29*, 102703. https://doi.org/10.1016/j.fochx.2025.102703
7. Rodríguez-Ortíz, D.; García-Moreira, D.P.; Vidaña, E.C.L.; Alanis, A.Y.; Moreno, I. Predicting Color Change in Solar-Dried Fruits Using Neural Networks: A Multilayer Perceptron Approach. *Journal of Stored Products Research* 2025, *115*, 102803. https://doi.org/10.1016/j.jspr.2025.102803
8. Tran, T.T.H.; Nguyen, T.T.D.; Kharaghani, A.; Le, K.H. Impact of Ultrasonic Pretreatment on Hot-Air Drying Kinetics and Quality of Carrot Slices: Simulations and Experimental Evaluation. *Appl. Sci.* 2023, *13*, 11865. https://doi.org/10.3390/app132111865
9. Suvanjumrat, C.; Kongsarai, K.; Phong-Arom, P.; Chumphong, N.; Promtong, M.; Priyadumkol, J. Development and Optimization of an Electrohydrodynamic Dehydrator Using ANN-GA for Improved Energy Performance. *Results in Engineering* 2025, *27*, 106049. https://doi.org/10.1016/j.rineng.2025.106049
10. Kaveh, M.; Sharabiani, V.R.; Chayjan, R.A.; Taghinezhad, E.; Abbaspour-Gilandeh, Y.; Golpour, I. ANFIS and ANN Models for Predicting Moisture Diffusivity and Specific Energy Consumption of Potato, Garlic, and Cantaloupe during Convective Hot-Air Drying. *Inf. Process. Agric.* 2018, *5*(3), 372–387. https://doi.org/10.1016/j.inpa.2018.05.003.
11. Chupawa, P.; Suksamran, W.; Jaisut, D.; Ronsse, F.; Duangkhamchan, W. Combined Heat and Mass Transfer Associated with Kinetic Models for the Analysis of Stepwise Convective Drying of Carrot Cubes. *Foods* 2022, *11*, 4045. https://doi.org/10.3390/foods11244045.
12. Shing, L.R.; Aranha, A.C.R.; De Souza Matias, G.; De Matos Jorge, L.M.; Sipoli, C.C.; Suzuki, R.M.; Gomes, M.C.S.; Sgorlon, J.G.; Defendi, R.O. Artificial Neural Networks in Separation Processes: Bibliometric Review and Predictive Modeling of Drying Kinetics. *Process Safety and Environmental Protection* 2025, *224*, 116–135. https://doi.org/10.1016/j.cherd.2025.11.003
13. Singh, H.; Goraya, R.K.; Singla, M.; Talwar, G.; Kumar, Y. Modeling and Optimization of Orange Peel Drying Using Thin-Layer Equations and Artificial Neural Networks for Standardized Powder Production. *Food Chemistry Advances* 2025, *9*, 101124. https://doi.org/10.1016/j.focha.2025.101124
14. Sharma, B.B.; Vaidya, P.; Kumar, N.; et al. Enhancing Postharvest Sustainability of Temperate Crops Using an IoT-Integrated Smart Indirect Solar Dryer. *Sci. Rep.* 2025, *15*, 28608. https://doi.org/10.1038/s41598-025-13499-x
15. Hmazi, F.A.; Bagar, H.; Madani, A.; Mrani, I. A Novel Approach for Modelling and Predicting the Drying Kinetics of Couscous Grains Using Artificial Neural Networks. *Journal of Food Composition and Analysis* 2024, *132*, 106301. https://doi.org/10.1016/j.jfca.2024.106301
16. Thanaboonrongkom, S.; Dajanta, K.; Chattong, U.; Sai-Ut, S.; Rawdkuen, S.; Onsaard, E.; Zhang, W.; Jung, Y.H.; Chaikham, P.; Jirasatid, S. Optimizing Quality, Functionality, and Safety of *Palmyrah* Palm (*Borassus flabellifer* Linn.) Pulp Powder via Steaming and Hot-Air Drying. *Appl. Food Res.* 2025, *5*(2), 101489. https://doi.org/10.1016/j.afres.2025.101489.
17. Mishra, N.; Jain, S.; Agrawal, N.; Jain, N.; Wadhawan, N.; Panwar, N. Development of Drying System by Using Internet of Things for Food Quality Monitoring and Controlling. *Energy Nexus* 2023, 11, 100219. https://doi.org/10.1016/j.nexus.2023.100219

 doi:10.20944/preprints202602.1525.v1

18. Wang, Q.; Wang, R.; Li, Z.; Zhao, Y.; Cao, Q.; Han, F.; Gao, Y. Kinetic, Thermodynamic and Artificial Neural Network Prediction Studies on Co-Pyrolysis of Agricultural Waste and Algae. *Renewable Energy* 2024, *233*, 121142. https://doi.org/10.1016/j.renene.2024.121142
19. Meerasri, J.; Sothornvit, R. Artificial Neural Networks (ANNs) and Multiple Linear Regression (MLR) for Prediction of Moisture Content for Coated Pineapple Cubes. *Case Studies in Thermal Engineering* 2022, *33*, 101942. https://doi.org/10.1016/j.csite.2022.101942
20. Parida, C.; Sahoo, P.K.; Nasir, R.; Waseem, L.A.; Tariq, A.; Aslam, M.; Hatamleh, W.A. Exergy Assessment of Infrared Assisted Air Impingement Dryer Using Response Surface Methodology, Back Propagation-Artificial Neural Network, and Multi-Objective Genetic Algorithm. *Case Studies in Thermal Engineering* 2023, *53*, 103936. https://doi.org/10.1016/j.csite.2023.103936
21. Sundarsingh, A.; BhagyaRaj, G.; Dash, K.K. Modeling and Optimization of Osmotic Dehydration of Wax Apple Slices Using Adaptive Neuro-Fuzzy Inference System. *Applied Food Research* 2023, *3*(2), 100316. https://doi.org/10.1016/j.afres.2023.100316
22. Barnard, J.E.; Chew, Y.J.; Perera, S.; Şimşek, Ö.; Balquis, K.; Barker, J. Accelerated Modelling of Moisture Diffusion Controlled Drying Using Coupled Physics-Informed Neural Network. *Food and Bioproducts Processing* 2024, *145*, 67–77. https://doi.org/10.1016/j.fbp.2024.02.004
23. Topal, M.E.; Şahin, B. Effects of Different Drying Methods on *Camellia sinensis*: Investigation of Quality Parameters and Drying Kinetics Using Artificial Neural Networks. *LWT* 2025, *229*, 118172. https://doi.org/10.1016/j.lwt.2025.118172
24. Leilayi, M.; Arabhosseini, A.; Akhijahani, H.S.; Kaveh, M.; Nezamlou, N.; Aghaei, M. Energy and Exergy Efficiencies of Batch Paddy Rice Drying with Liquefied Petroleum Gas Dehumidification: A Comprehensive Analysis Using Adaptive Neuro-Fuzzy Inference System and Artificial Neural Networks Approaches. *Energy Conversion and Management X* 2024, *25*, 100826. https://doi.org/10.1016/j.ecmx.2024.100826
25. Simonič, M.; Klančnik, S. Temporal and Statistical Perspectives on the Multivariate Forecasting of Maize Outlet Moisture in Continuous Flow Industrial Drying Systems. *Appl. Sci.* 2025, *15*, 9187. https://doi.org/10.3390/app15169187
26. Zuo, Y.; Jibril, A.N.; Yan, J.; Xia, Y.; Liu, R.; Chen, K. Optimization of the Online Moisture Prediction Model for Rice in a Low-Temperature Circulating Heat Pump Drying System Using an Artificial Neural Network. *Sensors* **2025**, 25, 2308. https://doi.org/10.3390/s25072308
27. Jia, Z.; Liu, Y.; Xiao, H. Deep Learning Prediction of Moisture and Color Kinetics of Apple Slices by Long Short-Term Memory as Affected by Blanching and Hot-Air Drying Conditions. *Processes* 2024, *12*, 1724. https://doi.org/10.3390/pr12081724
28. Yang, T.; Zheng, X.; Xiao, H.; Shan, C.; Yao, X.; Li, Y.; Zhang, J. Drying Temperature Precision Control System Based on Improved Neural Network PID Controller and Variable-Temperature Drying Experiment of Cantaloupe Slices. *Plants* 2023, *12*, 2257. https://doi.org/10.3390/plants12122257
29. Huang, X.; Li, Y.; Zhou, X.; Wang, J.; Zhang, Q.; Yang, X.; Zhu, L.; Geng, Z. Prediction of Apple Slices Drying Kinetic during Infrared-Assisted Hot Air Drying by Deep Neural Networks. *Foods* 2022, *11*, 3486. https://doi.org/10.3390/foods11213486
30. Li, B.; Li, C.; Huang, J.; Li, C. Application of Artificial Neural Network for Prediction of Key Indexes of Corn Industrial Drying by Considering the Ambient Conditions. *Appl. Sci.* 2020, *10*, 5659. https://doi.org/10.3390/app10165659
31. Francik, S.; Łapczyńska-Kordon, B.; Hajos, M.; Basista, G.; Zawiślak, A.; Francik, R. Modeling the Drying Process of Onion Slices Using Artificial Neural Networks. *Energies* 2024, *17*, 3199. https://doi.org/10.3390/en17133199
32. Zhang, Y.; Jin, W.; Chen, X.; Wang, Y.; Zeng, Q. Effects of Hot-Air Drying Conditions on Quality Attributes of Meat and Shell of Dried Shrimp. *Foods* 2025, *14*, 4041. https://doi.org/10.3390/foods14234041
33. Chang, K.; Li, J.; Jin, Y.; Liu, C. Development of Grain Dryer Control Technology from the Perspective of Low Carbon and Intelligentization. *Appl. Sci.* 2024, *14*, 10587. https://doi.org/10.3390/app142210587

 doi:10.20944/preprints202602.1525.v1

34. Liu, Z.; Xu, Y.; Han, F.; Zhang, Y.; Wang, G.; Wu, Z.; Wu, W. Control Method for Continuous Grain Drying Based on Equivalent Accumulated Temperature Mechanism and Artificial Intelligence. *Foods* 2022, *11*, 834. https://doi.org/10.3390/foods11060834
35. Pang, S.; Jia, J.; Ding, X.; Yu, S.; Liu, Y. Intelligent Control in the Application of a Rotary Dryer for Reduction in the Over-Drying of Cut Tobacco. *Appl. Sci*. 2021, 11, 8205. https://doi.org/10.3390/app11178205
36. Sanchez-Chero, M.; Miranda-Zamora, W.R.; Flores-Mendoza, L.C.; Sanchez-Chero, J. Development of a PLC/IoT Control System with Real-Time Concentration Monitoring for the Osmotic Dehydration of Fruits. *Automation* 2025, 6, 68. https://doi.org/10.3390/automation6040068
37. Mansour, N.E.; Villagran, E.; Rodriguez, J.; Akrami, M.; Flores-Velazquez, J.; Metwally, K.A.; Alhumedi, M.; Ahmed, A.F.; Elwakeel, A.E. Effect of Drying Conditions on Kinetics, Modeling, and Thermodynamic Behavior of Marjoram Leaves in an IoT-Controlled Vacuum Dryer. *Sustainability* 2025, 17, 5980. https://doi.org/10.3390/su17135980
38. Hoque, A.; Roy, S.; Padhiary, M.; Prasad, G.; Swain, B.; Saikia, P.; Saha, D. Integrating Remote Sensing and AI in Smart Greenhouse Solar Dryers: Enhancing Efficiency, Traceability, and Sustainability in the Drying of Fruits and Spices. *J. Agric. *Food Res.* 2025, 23, 102310. https://doi.org/10.1016/j.jafr.2025.102310
39. Rana, M.M.; Asdaria, R.; Mahmud, S.; Irfan, A.F.; Chowdhury, A.J.K.; Munir, M.B. Marine Water Aquaculture and an IoT-Based Smart Fish Dryer of the Future: A Sustainable Environmental Approach. *Desalination Water Treat*. 2023, 315, 515–522. https://doi.org/10.5004/dwt.2023.30017
40. Villa-Medina, J.F.; Porta-García, M.Á.; Gutiérrez, J.; Porta-Gándara, M.Á. Solar Forced Convection Dryer for Agriproducts Monitored by IoT. *Internet Things* 2025, 31, 101566. https://doi.org/10.1016/j.iot.2025.101566
41. Martins, P.; Cláudio, R.; Soares, F.; Leitão, J.; Váz, P.; Silva, J.; Abbasi, M. Intelligent Control System for Wood Drying: Scalable Architecture, Predictive Analytics, and Future Enhancements. Procedia Comput. *Sci*. **2024**, 238, 602–609. https://doi.org/10.1016/j.procs.2024.06.067
42. Naniwadekar, M.; Walke, S.; Mandake, M.; Tapre, R.; Patil, K.; Komble, S. A Comprehensive Study of Performance Metrics and Potato Dehydration at Various Slice Thickness Using an IoT-Based Indirect Solar Dryer: An Experimental Approach. *Sol. Energy* 2025, 288, 113269. https://doi.org/10.1016/j.solener.2025.113269
43. Hu, Z.; Zhang, X.; Workneh, T.S. Optimisation and Enhancement of the Physicochemical and Phytochemical Properties of Dried Okra, Using a Self-Organising Map and Developing an Artificial Intelligence Prediction Model: Microwave-Assisted Convective Drying Technique. *LWT* **2025**, 238, 118836. https://doi.org/10.1016/j.lwt.2025.118836
44. Mahda, M.; Rajathi, K.; Elangovan, M.; Kumar, S.P.; Verma, A. Experimental Investigation of Solar PVT Collector with the Dryer on Mass and Temperature of Dried Red Chili with Machine Learning Models. *Results Eng*. **2025**, 27, 105827. https://doi.org/10.1016/j.rineng.2025.105827
45. Bannoud, M.A.; Gomes, B.P.; Abdalla, M.C.S.P.; et al. Mathematical Modeling of the Drying Kinetics of Milled Açaí (*Euterpe oleracea*) Using Artificial Neural Networks. *Chem. Pap.* 2024, *78*, 1033–1054. https://doi.org/10.1007/s11696-023-03142-2
46. Tepe, T.K.; Tepe, F.B. Improvement of Pear Slice Drying through Pretreatments and Microwave-Assisted Convective Drying: Drying Characteristics, Artificial Neural Network Modeling, and Principal Component Analysis of Quality Parameters. *J. Therm. Anal. Calorim.* 2024, *149*, 7313–7328. https://doi.org/10.1007/s10973-024-13280-8.
47. Gite, S.S.; Kaushik, A.; Singh, S. Artificial Neural Network Modeling of Drying Kinetics of Wild Bitter Gourd during Hot-Air Drying. *J. Biosyst. Eng.* 2025, *50*, 310–328. https://doi.org/10.1007/s42853-025-00268-x
48. Davari, O.; Rafati, A.; Nosrati, M.; et al. Leveraging Artificial Neural Networks for Real-Time Monitoring of Moisture Gradient during Brown Rice Drying Using a Combined Hot-Air and Far-Infrared Dryer. *Food Anal. Methods* 2026, *19*, 36. https://doi.org/10.1007/s12161-025-02944-2.
49. Tejeda Miramontes, J.P.; Galarza Andrade, I.J.; Escalante González, J.A.; Tejada Ortigoza, V.; García Cayuela, T.; Garcia Amezquita, L.E. Phase-Segmented Analysis of Blackberry Pomace Convective Drying:

 doi:10.20944/preprints202602.1525.v1

Mass Transfer Dynamics, Exergy Efficiency, and Staged Temperature Guidelines. *LWT* 2025, *233*, 118509. https://doi.org/10.1016/j.lwt.2025.118509

50. Gebeyehu, S.K.; Asemu, A.M.; Haile, A.S.; Kassa, M.G. Influence of Temperature and Mango Pulp Thickness on the Performance of Batch Window Refractance Dryer. *Appl. Food Res*. **2025**, 5, 100939. https://doi.org/10.1016/j.afres.2025.100939
51. Kalinke, I.; Röder, J.; Unterbuchberger, G.; Kulozik, U. Microwave-Assisted Freeze Drying: The Role of Power Input and Temperature Control on Energy Efficiency and Uniformity. *J. Food Eng*. **2024**, 390, 112410. https://doi.org/10.1016/j.jfoodeng.2024.112410
52. Ramachandran, R.P.; Nadimi, M.; Cenkowski, S.; et al. Advances and Innovations in the Drying of Biopharmaceutical, Nutraceutical, and Functional Food Products. *Food Eng. Rev.* 2024, *16*, 540–566. https://doi.org/10.1007/s12393-024-09381-7
53. Selvakumarasamy, S.; Kulathooran, R.; Rengaraju, B. Effect of Drying on Insulin Plant Leaves for Sustainability and Modeling of Drying Kinetics Using Mathematical Models and Artificial Neural Networks. *Environ. Model. Assess.* 2024, *29*, 901–914. https://doi.org/10.1007/s10666-024-09974-w
54. Tepe, T.K. Convective Drying of Golden Delicious Apple Enhancement: Drying Characteristics, Artificial Neural Network Modeling, Chemical and ATR-FTIR Analysis of Quality Parameters. *Biomass Conv. Bioref.* 2024, *14*, 13513–13531. https://doi.org/10.1007/s13399-024-05562-w
55. Liu, X.; Grasso-Kelley, E.M.; Lee, A.; Warda, L.; Anderson, N.M. Salmonella spp. Inactivation During Hot Air Drying of Apples: Influence of Temperature, Bed Depth, and Air Velocity. *J. Food Prot*. **2025**, 88, 100597. https://doi.org/10.1016/j.jfp.2025.100597
56. Yu, M.; Zou, L.; Yu, J. Experimental Investigation on the Drying Characteristics in a Solar Assisted Ejector Enhanced Heat Pump Dryer System. *Solar Energy* **2024**, 267, 112265. https://doi.org/10.1016/j.solener.2023.112265
57. Susana, I.G.B.; Alit, I.B.; Okariawan, I.D.K. Rice Husk Energy Rotary Dryer Experiment for Improved Solar Drying Thermal Performance on Cherry Coffee. Case Stud. *Therm. Eng*. **2023**, 41, 102616. https://doi.org/10.1016/j.csite.2022.102616
58. Hamdani, N.; Rizal, T.; Muhammad, Z. Fabrication and testing of hybrid solar-biomass dryer for drying fish. Case Stud. *Therm. Eng*. **2018**, 12, 489–496. https://doi.org/10.1016/j.csite.2018.06.008
59. Soponpongpipat, N.; Nanetoe, S.; Comsawang, P. Thermal and Torrefaction Characteristics of a Small-Scale Rotating Drum Reactor. *Processes* **2020**, 8, 489. https://doi.org/10.3390/pr8040489
60. Yang, G.; Yang, X.; Li, C.; Wei, X.; Lu, Z.; Zhang, C.-A.; Wang, Q.; Wu, X. Numerical Study on the Uniform Distribution of Flow Field of Airflow Dryer. *Heliyon* **2024**, 10, e29439. https://doi.org/10.1016/j.heliyon.2024.e29439
61. van Boven, A.P.; Dubbelboer, A.; Janssen, T.J.A.; Schröder, J.; Sewalt, J.J.W.; Kohlus, R.; Schutyser, M.A.I. Investigating the Impact of Air Distribution on Spray Dryer Operability Using CFD Simulations and Pilot-Scale Experiments. *Powder Technol*. **2024**, 440, 119779. https://doi.org/10.1016/j.powtec.2024.119779
62. Charmongkolpradit, S.; Somboon, T.; Phatchana, R.; Sang-Aroon, W.; Tanwanichkul, B. Influence of drying temperature on anthocyanin and moisture contents in purple waxy corn kernel using a tunnel dryer. *Case Stud. Therm. Eng*. **2021**, *25*, 100886. https://doi.org/10.1016/j.csite.2021.100886
63. Wang, Y.; Ding, C. Effect of Electro hydrodynamic Drying on Drying Characteristics and Physicochemical Properties of Carrot. *Foods* **2023**, *12*, 4228. https://doi.org/10.3390/foods12234228
64. Adegbite, S.A.; Asiru, W.B.; Sartas, M.; Tran, T.; Taborda, A.L.; Chapuis, A.; Ojide, M.; Abass, A. Development of a Pilot Scale Energy Efficient Flash Dryer for Cassava Flour. *Resour. Environ. Sustain.* **2023**, *13*, 100117. https://doi.org/10.1016/j.resenv.2023.100117
65. AitHmazi, O.; Bagar, H.; Madani, A.; Mrani, I. A Novel Approach for Modelling and Predicting the Drying Kinetics of Couscous Grains Using Artificial Neural Networks. *J. Food Compos. Anal.***2024**, *132*, 106301. https://doi.org/10.1016/j.jfca.2024.106301
66. Dash, K.K.; Sundarsingh, A.; BhagyaRaj, G.V.S.; Pandey, V.K.; Kovács, B.; Mukarram, S.A. Modelling of Ultrasonic Assisted Osmotic Dehydration of Cape Gooseberry Using Adaptive Neuro-Fuzzy Inference System (ANFIS). Ultrason. Sonochem. **2023**, 96, 106425. https://doi.org/10.1016/j.ultsonch.2023.106425

 doi:10.20944/preprints202602.1525.v1

67. Mierzwa, D.; Musielak, G. Microwave and Ultrasound Assisted Rotary Drying of Carrot: Analysis of Process Kinetics and Energy Intensity. Appl. Sci. **2024**, 14, 10676. https://doi.org/10.3390/app142210676
68. El-Mesery, H.S.; Ali, M.; Qenawy, M.; Adelusi, O.A. Application of Artificial Intelligence to Predict Energy Consumption and Thermal Efficiency of Hybrid Convection-Radiation Dryer for Garlic Slices. Eng. Appl. Artif. Intell. **2024,** 138, 109338. https://doi.org/10.1016/j.engappai.2024.109338
69. Li, M.; Liu, M.; Xu, C.; Wang, J.; Yan, J. Thermodynamic and Sensitivity Analyses on Drying Subprocesses of Various Evaporative Dryers: A Comparative Study. Energy 2023, 284, 128571. https://doi.org/10.1016/j.energy.2023.128571
70. Tabares-Martinez, J.M.; Guzmán-López, A.; Bravo-Sánchez, M.G.; Aceves, S.M.; Pantoja-Pacheco, Y.V.; Aguilera-Álvarez, J.P. Evaluation of a Cyber-Physical System with Fuzzy Control for Efficiency Optimization in Rotary Dryers: Real-Time Multivariate Monitoring of Humidity, Temperature, Air Velocity and Mass Loss. *Technologies* 2025, *13*(9), 424. https://doi.org/10.3390/technologies13090424
71. Kang, C.; Zhang, G.; Mu, G.; Guo, H.; Yuan, T.; Zhao, C.; Li, X.; Zhang, Q. Solar-Heat Pump Combined Drying with Phase Change Heat Storage: Multi-Energy Self-Adaptive Control. Renew. Energy **2024**, 230, 120867. https://doi.org/10.1016/j.renene.2024.120867
72. Vega-Gálvez, A.; Orellana-Palma, P.; Pasten, A.; Uribe, E.; Cortés, D.; Carvajal, M. Mild Temperature Conditions Applied to Carrot (Daucus carota L.) Waste Using Different Drying Methods: Effect on the Kinetics and Some Chemical Parameters. Processes **2025**, 13, 90. https://doi.org/10.3390/pr13010090
73. Tabares-Martinez, J.M.; Guzmán-López, A.; Bravo-Sánchez, M.G.; Barranco-Gutierrez, A.I.; Martínez-Nolasco, J.J.; Villaseñor-Ortega, F. Instrumentation and Evaluation of a Sensing System with Signal Conditioning Using Fuzzy Logic for a Rotary Dryer. *Technologies* 2025, *13*(2), 83. https://doi.org/10.3390/technologies13020083